



UNIVERSITI  
TEKNOLOGI  
MARA

# Journal of Mechanical Engineering

*An International Journal*

Volume 12 No. 1

June 2015

ISSN 1823-5514

---

Investigation on Heat Transfer Characteristics  
of Ceramic Coated Piston Crown for a CNGDI Engines

Helmisyah Ahmad Jalaludin

---

Accuracy Improvement for Linear Tetrahedral Finite  
Element by Means of Virtual Mesh Refinement

Sugeng Waluyo

---

Two-Dimensional Fast Lagrangian Vortex Method for  
Simulating Flows around a Moving Boundary

Duong Viet Dung  
Lavi R. Zuhail  
Hari Muhammad

---

Simulation Analysis of the Effect of Temperature on  
Overpotentials in PEM Electrolyzer System

A.H. Abdol Rahim  
Alhassan Salami Tijani  
Farah Hanun Shukri

---

The Effect of Skin Orientation on Biomechanical Properties

Nor Fazli Adull Manan  
Jamaluddin Mahmud

---

A Study of Single and Two-Plane Balancing  
Using Influence Coefficient Method

Wan Sulaiman Wan Mohamad  
A. A. Mat Isa  
M.A Ismail

---

# JOURNAL OF MECHANICAL ENGINEERING (JMechE)

## EDITOR IN CHIEF:

Professor Wahyu Kuntjoro – Universiti Teknologi  
MARA, Malaysia

## EDITORIAL BOARD:

Datuk Professor Ow Chee Sheng – Universiti  
Teknologi MARA, Malaysia

Dr. Ahmad Azlan Mat Isa – Universiti Teknologi  
MARA, Malaysia

Dr. Faqir Gul – Institute Technology Brunei,  
Brunei Darussalam

Dr. Mohd. Afian Omar – SIRIM Malaysia

Dr. Valliyappan David a/l Natarajan – Universiti  
Teknologi MARA, Malaysia

Dr. Yongki Go Tiau Hiong – Florida Institute  
of Technology, USA

Professor Abdelmagid Salem Hamouda – Qatar  
University, Qatar

Professor Abdul Rahman Omar – Universiti  
Teknologi MARA, Malaysia

Professor Ahmed Jaffar – Universiti Teknologi  
MARA, Malaysia

Professor Bernd Schwarze – University of  
Applied Science, Osnabrueck, Germany

Professor Bodo Heimann – Leibniz University  
of Hannover Germany

Professor Darius Gnanaraj Solomon – Karunya  
University, India

Professor Dr. Hazizan Md. Akil – Universiti  
Sains Malaysia, Malaysia

Professor Dr. Mohd. Zulkifly Abdullah –  
Universiti Sains Malaysia, Malaysia

Professor Dr. Roslan Abd. Rahman – Universiti  
Teknologi Malaysia, Malaysia

Professor Dr. Salmiah Kasolang – Universiti  
Teknologi MARA, Malaysia

Professor Essam E. Khalil – University of Cairo,  
Egypt

Professor Ichsans S. Putra – Bandung Institute of  
Technology, Indonesia

Professor Ir. Dr. Shahrir Abdullah – Universiti  
Kebangsaan Malaysia

Professor Ir. Dr. Shahrum Abdullah – Universiti  
Kebangsaan Malaysia

Professor Masahiro Ohka – Nagoya University,  
Japan

Professor Miroslaw L. Wyszynski – University of  
Birmingham, UK

Professor Mohamad Nor Berhan – Universiti  
Teknologi MARA, Malaysia

Professor P. N. Rao – University of Northern  
Iowa, USA

Professor Wirachman Wisnoe – Universiti  
Teknologi MARA, Malaysia

Professor Yongtae Do – Daegu University, Korea

## EDITORIAL EXECUTIVES:

Assoc. Prof. Dr. Solehuddin Shuib

Dr. Muhad Rozi Mat Nawi

Dr. Noor Azlina Mohd Salleh

Dr. Siti Mariam Abdul Rahman

Nurul Hayati Abdul Halim

Rosnadiyah Bahsan

Copyright © 2015 by the Faculty of Mechanical Engineering (FKM), Universiti Teknologi MARA, 40450 Shah Alam, Selangor, Malaysia.

All rights reserved. No part of this publication may be reproduced, stored in a retrieval system, or transmitted in any form or any means, electronic, mechanical, photocopying, recording or otherwise, without prior permission, in writing, from the publisher.

*Journal of Mechanical Engineering (ISSN 1823-5514) is published by the Faculty of Mechanical Engineering (FKM) and UiTM Press, Universiti Teknologi MARA, 40450 Shah Alam, Selangor, Malaysia.*

*The views, opinions and technical recommendations expressed herein are those of individual researchers and authors and do not necessarily reflect the views of the Faculty or the University.*

# Journal of Mechanical Engineering

*An International Journal*

Volume 12 No. 1

June 2015

ISSN 1823-5514

1. Investigation on Heat Transfer Characteristics of Ceramic Coated Piston Crown for a CNGDI Engines 1  
*Helmisyah Ahmad Jalaludin*
2. Accuracy Improvement for Linear Tetrahedral Finite Element by Means of Virtual Mesh Refinement 19  
*Sugeng Waluyo*
3. Two-Dimensional Fast Lagrangian Vortex Method for Simulating Flows around a Moving Boundary 31  
*Duong Viet Dung*  
*Lavi R. Zuhail*  
*Hari Muhammad*
4. Simulation Analysis of the Effect of Temperature on Overpotentials in PEM Electrolyzer System 47  
*A.H. Abdol Rahim*  
*Alhassan Salami Tijani*  
*Farah Hanun Shukri*
5. The Effect of Skin Orientation on Biomechanical Properties 67  
*Nor Fazli Adull Manan*  
*Jamaluddin Mahmud*

6. A Study of Single and Two-Plane Balancing Using Influence  
Coefficient Method

83

*Wan Sulaiman Wan Mohamad*

*A. A. Mat Isa*

*M. A Ismail*

# Simulation Analysis of the Effect of Temperature on Overpotentials in PEM Electrolyzer System

*A.H. Abdol Rahim*

*Alhassan Salami Tijani*

*Farah Hanun Shukri*

*Faculty of Mechanical Engineering*

*Universiti Teknologi MARA, Shah Alam*

*Selangor, Darul Ehsan Malaysia*

## ABSTRACT

*Mass transport through the porous electrode of Polymer Electrolyte Membrane (PEM) electrolyzer encounters a resistance when it flows through the electrodes. As the resistance increases with increasing flow, some energy is lost in the process which causes diffusion overvoltage. The cell voltage to be imposed is higher because of mass transport limitations. In PEM electrolyzer, the cell voltage is generally the sum of reversible voltage and the overpotentials. The ohmic, activation and mass transfer losses are the most prominent losses in a PEM electrolyzer. In this manuscript, mathematical models related to PEM electrolyzer based on a combination of thermodynamics fundamental and electrochemical relations are presented. A single cell simple PEM electrolyzer is analyzed on the basis of well-known Butler-Volmer kinetic for electrodes and transport resistance in the polymer-electrolyte. In addition, the overpotential at the anode, cathode and overpotential due to ohmic resistances are analyzed as well. Then, the effect of temperature on operating cell voltage, resistance and ionic conductivity of the polymer electrolyte are examined with the developed model. Finally sensitivity analysis for different values of exchange current densities at anode and cathode are tested. The simulation results indicated that as temperature increases, there is a significant or sharp decrease in ohmic resistance from  $0.198\Omega/\text{cm}^2$  at  $40^\circ\text{C}$  to  $0.125\Omega/\text{cm}^2$  at  $80^\circ\text{C}$ . Also at  $40^\circ\text{C}$  and  $2\text{A}/\text{cm}^2$ , an operating voltage of  $2.13\text{V}$  has been achieved, however at higher temperature ( $80^\circ\text{C}$ ), the operating cell voltage drops to  $1.98\text{V}$  at  $2\text{A}/\text{cm}^2$  and this constitutes about 7% reduction in*

*operating cell voltage. From this observation it can be concluded that the ionic conductivity of the membrane assembly increases with temperature.*

**Keywords:** *Renewable energy, PEM electrolyzer, hydrogen production, overpotentials*

## **Introduction**

Conventional energy resources are currently important factors that contribute to the development of a nation especially in the industrial sector. However due to increasing global energy demand, the fossil fuel reserves such as coal natural gas and petroleum are depleting at an alarming rate. Recently, there have been a lot of concern and challenges among researchers and stakeholders in the energy sector to meet the global energy demand. Fossil fuels such as coal and methane are known to emit carbon dioxide into the atmosphere which is responsible for global warming effects. It is therefore important to look for other more reliable and sustainable energy sources. One of the alternative energy sources such as hydrogen has been introduced to replace conventional energy sources. It contributes towards more sustainable, environmental friendly criteria, energy economy and energy carrier in the future [1, 2]. It is one of the potential solutions to the current energy and environmental pollution crises due to its carbon free [2].

Currently hydrogen energy production through advanced technologies using energy resources from fossils is 95% in particular by steam reforming of natural gas (48%) [3]. According to Simon et al. [4] hydrogen production from other fossil fuel resources (Hydrocarbon 30% and Coal 18%) is primarily obtained by the process of partial oxidation. Nowadays, they have many technologies of hydrogen production produce from renewable energy sources for hydrogen production that offer a promising “green-hydrogen”. These technologies are advanced alkaline electrolyzer, photoelectrochemical and PEM electrolyzer technologies. The most advanced process of hydrogen production from renewable energy source is by the electrolysis of pure alkaline water as a raw material which allows to response 4% of the world’s demand in hydrogen energy [3]. Figure 1 below shows the distribution of the modes of hydrogen production. PEM electrolyzer offers an efficient, flexible and practicality for a high quality of hydrogen production [5, 6]. It is a device involving the process of water splitting molecules into hydrogen and oxygen gas using electrical power and its bases on electrochemical process. In recent times more attention is being paid to PEM electrolyzer as it offers several advantages compared other method of electrolysis in terms of smaller mass volume characteristic, higher in current densities, high degree of gas purity and better safety level [7]. Operated based on a low-temperature 40° – 80°C [8], Antonucci et al [9] found the performance

of PEM electrolyzer where Nafion 115 as a membrane drastically decreased by increasing the temperature up to 120°C. By increasing the temperature from 20° to 60°C the exchange current density at the anode decreased which gives significant change in the temperature dependence of the exchange current density at the anode [10].

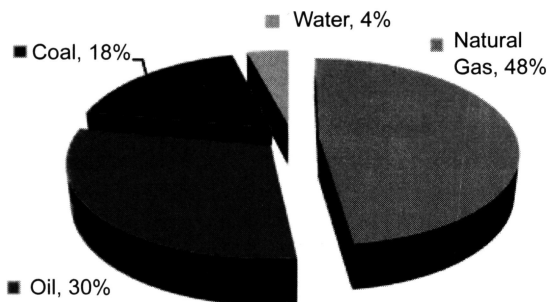
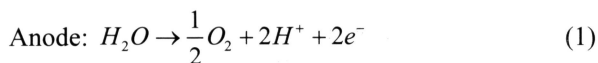


Figure 1: Distribution of the modes of hydrogen production

## Mode of Operation for (PEM) Electrolyzer System

A PEM electrolyzer cell is composed of an anode chamber, a cathode chamber, two electrode catalyst surfaces and a proton exchange membrane [11]. The dissociation of water into hydrogen and oxygen is relatively high since water molecules have a stable structure at ambient temperature [12]. A minimum potential of 1.23V (reversible voltage) is applied across the electrochemical cell to initiate electrochemical reactions at both anode and cathode electrodes. Water is introduced at the anode (see Figure 2) and dissociated into oxygen, protons and electrons via the following reaction:



The hydrogen ions are driven through the membrane to the cathode under an electric field where they combine with the electrons arriving from the external circuit to form hydrogen gas:



The net reaction for entire cell is:



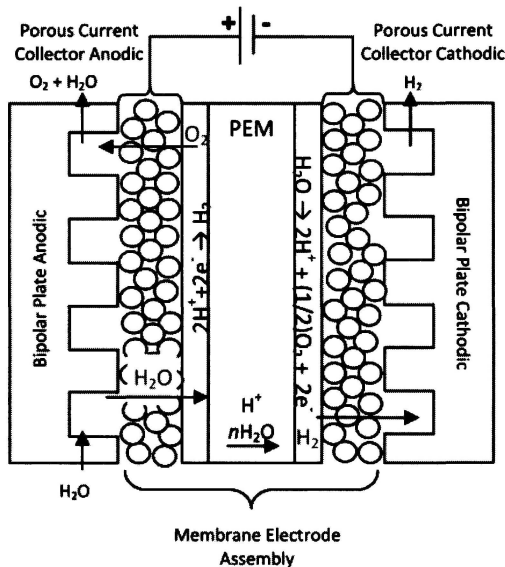


Figure 2: Basic schematic of a PEM water electrolyzer cell

## Methods and Mathematical Modeling

### Operating cell voltage

A single operating cell voltage of PEM electrolyzer is given by the summation of the reversible voltage and the other different overpotentials [13];

$$V_{cell} = V_{rev} + \eta_{act} + \eta_{\Omega} \quad (4)$$

### Reversible voltage

Each reaction at the electrodes depends on the reactions of water at minimum voltage which corresponds to the reversible potential. This can be determined by using the Gibbs free energy equation [14];

$$\Delta G = \eta F V_{rev} \quad (5)$$

$$V_{rev} = \frac{\Delta G}{\eta F} \quad (6)$$

Where  $\Delta G$  is the Gibbs free energy of 237.178 kJ/K.mole (also known as the lower heating value, (LHV)),  $V_{rev}$  is the reversible voltage,  $\eta$  is the number

of the electrons and  $F$  is the Faraday's Constant. Since all variables in equation (6) are already known, the value of the reversible voltage of the cell can be calculated as [13];

$$V_{rev} = \frac{237.178 \frac{kJ}{K.mole}}{2 \times 96485.3 \frac{columbs}{mole}} = 1.229V \quad (7)$$

### **Thermoneutral voltage**

In thermodynamic of electrolysis, since the Gibbs free energy is known as the maximum amount of usable electrical energy available when the hydrogen recombines with the oxygen, the thermoneutral voltage can be identified as the amount of the energy losses in the electrolysis system. The thermoneutral voltage can be identified as [13];

$$V_m = \frac{\Delta H^0}{\eta F} \quad (8)$$

where  $\Delta H^0$  is the high heating value (HHV) of 285.84 kJ/K.mole. The value of the thermoneutral voltage can be clarified as [13];

$$V_m = \frac{285.4 \frac{kJ}{K.mole}}{2 \times 96485.3 \frac{columbs}{mole}} = 1.481 \text{ Volt / cell} \quad (9)$$

Since the value of thermoneutral voltage is the amount of energy losses in the cell, it will not be included in Equation (4) to get the cell voltage values.

### **Activation overvoltage**

By relating the Butler-Volmer expression, the current density at the anode and cathode can be expressed in terms of charge transference phenomena and exchange current density. The current density at anode [15];

$$i_a = i_{o,a} \left[ \exp\left(\frac{\alpha_1 \eta F}{RT} \eta_a\right) - \exp\left(-\frac{\alpha_2 \eta F}{RT} \eta_a\right) \right] \quad (10)$$

The current density at cathode [15];

$$i_c = i_{o,c} \left[ \exp\left(-\frac{\alpha_2 \eta F}{RT} \eta_c\right) - \exp\left(-\frac{\alpha_1 \eta F}{RT} \eta_c\right) \right] \quad (11)$$

where  $R$  is the universal gas constant,  $R = 8.314 \text{ J/mol.K}$ ,  $T$  is the variable temperature,  $T(\text{K})$ ,  $\alpha_1$  and  $\alpha_2$  are the symmetry factors which at the anode represent additional energy fraction of the reduction whereas the cathode represent the oxidation.  $\eta$  is the number of electrons involved. Moreover, the activation overpotentials at anode and cathode can be inscribed as [13];

$$\eta_a = \frac{RT}{\alpha_a zF} \ln \left( \frac{i_a}{i_{o,a}} \right) \quad (12)$$

$$\eta_c = -\frac{RT}{\alpha_c zF} \ln \left( \frac{i_c}{i_{o,c}} \right) \quad (13)$$

where  $z$  is the stoichiometric coefficient of the number of electrons involved,  $\alpha_a$  and  $\alpha_c$  are the charge transfer coefficients. The values of  $\alpha_a$  and  $\alpha_c$  are 0.5 on the symmetry reactions. The value of the stoichiometric coefficient is 2 since it was water electrolysis.

The value of the exchange current density at anode,  $i_{o,a}$ , and cathode,  $i_{o,c}$ , can give a very high impact on the activation overpotential values on both sides. By expressing the Arrhenius equation, the value of each exchange current density at anode and cathode can be identified using these equations [15];

$$i_{o,a} = i_{o,a}^{ref} \exp \left( -\frac{EA_a}{R} \left( \frac{1}{T} - \frac{1}{T_0} \right) \right) \quad (14)$$

$$i_{o,c} = i_{o,c}^{ref} \exp \left( -\frac{EA_c}{R} \left( \frac{1}{T} - \frac{1}{T_0} \right) \right) \quad (15)$$

where  $T_0$  is the reference temperature,  $T_0 (\text{K})$ ,  $EA_a$  and  $EA_c$  are the anodic and cathodic active energy ( $\text{J/mol}$ ), also  $i_{o,a}^{ref}$  and  $i_{o,c}^{ref}$  are the anodic and the cathodic reference exchange current density at reference temperature  $T_0$ . The role of activation overpotential can be derived as [13];

$$\eta_{act} = \eta_a + |\eta_c| \quad (16)$$

By referring an example from Choi et al. [15] they suggested that the exchange current densities at anode, cathode based on Platinum electrode catalyst and platinum iridium electrode catalyst referred on the parameters given in Table 1.

Table 1: Model parameter model parameters for water electrolysis for Pt based anode and cathode electrodes on Nafion® electrolyte [15, 16]

Parameters	Values	Dimension	References
$i_{0,a}$ , Pt	$10^{-12} - 10^{-9}$	A/cm <sup>2</sup>	Platinum electrode catalyst
$i_{0,a}$ , Pt - Ir	$10^{-7}$	A/cm <sup>2</sup>	Platinum iridium electrode catalyst
$i_{0,c}$ , Pt	$10^{-4} - 10^{-3}$	A/cm <sup>2</sup>	Platinum electrode catalyst

### Ohmic overvoltage

The ohmic overpotential can be classified into two categories:

- i. Ohmic overpotential due to membrane resistance (ionic resistance).  
This is caused by the membrane resistance to the flow of ions. It is also called voltage drop due to membrane resistance to the flow of ions. This can be expressed as [15];

$$\eta_{\Omega,mem} = \frac{\varphi}{\sigma} i \quad (17)$$

where  $R_{ion} = \frac{\varphi}{\sigma}$  is an ionic resistance as a function of membrane thickness conductivity,  $\varphi$  is the membrane height, (cm), and  $\sigma_{mem}$  is the local ionic conductivity with water content and temperature function. This can be written as [15];

$$\sigma_{mem} = (0.005139\lambda - 0.00326) \exp \left[ 1268 \left( \frac{1}{303} - \frac{1}{T_{cell}} \right) \right] \quad (18)$$

where  $\lambda$  is the degree of membrane humidification.

- ii. Interfacial overpotential (electronic resistance).  
This is caused by electronic materials such as bipolar plates, electrodes current collectors, etc. The interfacial resistance can be expressed as [13];

$$\eta_{\Omega,e} = R_{ele} i \quad (19)$$

The ohmic resistance of the electronic materials is;

$$R_{ele} = \frac{\rho l}{A} \quad (20)$$

where,  $\rho$  is the material resistivity ( $\Omega m$ ),  $l$  is the length of the electrons path and  $A$  is the conductor cross-sectional area. The ohmic overpotential due to electronic and ionic resistances is [13];

$$\eta_{\Omega, mem} = (R_{ele} + R_{ion})i \quad (21)$$

The value of activation overpotential at the anode and cathode can be calculated using Equation (12) and Equation (13), using all parameters related in Table 2.

Table 2: Parameter selection in ohmic

Parameters	Values	Unit
$i_{o,a}$	$10^{-9}$	A/cm <sup>2</sup>
$i_{o,c}$	$10^{-3}$	A/cm <sup>2</sup>
$R_{ele}$	0.035	m $\Omega$
$t_{mem}$	200	$\mu m$
$\lambda$	17	-

### Diffusion overvoltage

The diffusions give a function in overcoming energy loss presume in the cell due to the mass transport resistance of electrochemical reaction in the interface of the membrane and electrode [13]. Considering the value of the diffusions is so small and may not give major impact on the simulation result, it can be neglected. Finally, from Equation (4), the overall operating cell voltage can be concluded as;

$$V_{cell} = V_{rev} + \frac{RT}{\alpha_a zF} \ln \left( \frac{i_a}{i_{o,a}} \right) + \left| -\frac{RT}{\alpha_c zF} \ln \left( \frac{i_c}{i_{o,c}} \right) \right| + \left( R_{ele} + \frac{t_{mem}}{(0.005139\lambda - 0.00326) \exp \left[ 1268 \left( \frac{1}{303} - \frac{1}{T_{cell}} \right) \right]} \right) i \quad (22)$$

### Molar flow rate

It is known that the current  $I$ , can be found using [15];

$$I = iA \quad (23)$$

where,  $I$  is the current density and  $A$  is the electrode area. By governing the Faraday's law in this electrochemical cell, the molar flow rate related can be written as [13];

$$H_2 = \frac{\eta_{cell} I}{2F} \eta_F \quad (24)$$

$$O_2 = \frac{\eta_{cell} I}{4F} \eta_F \quad (25)$$

$$H_2O = 1.25 \frac{\eta_{cell} I}{2F} \eta_F \quad (26)$$

The number of electrolytic cells used is only one cell, thus  $\eta_{cell} = 1$ , while  $I$  is the overall current across the cell. The Faraday efficiency,  $\eta_F$ , is the differential between the experimental and theoretical hydrogen flow rate. It can be assumed as 100% since many other literatures agreed with 95% [13]. Since this was explained, the Equation (24), (25) and (26) can be simplified to be [14];

$$\dot{\eta}H_2 = \frac{I}{2F} \quad (27)$$

$$\dot{\eta}O_2 = \frac{I}{4F} \quad (28)$$

$$\dot{\eta}H_2O = 1.25 \frac{I}{2F} \quad (29)$$

The hydrogen production can be expressed in terms of volume flowrate;

$$\dot{Q}_H = \dot{\eta}H_2 \left( \frac{mol}{s} \right) \times \left( \frac{3600s}{1hr} \right) \times \left( \frac{0.022414m^3}{mol} \right) = \frac{m^3}{hr} \quad (30)$$

The hydrogen volume flowrate can be converted to L/min as shown below.

$$Q = \frac{m^3}{hr} \times \frac{1hr}{60 \min} \times \frac{1000L}{1m^3} = \frac{L}{\min} \quad (31)$$

## Results and Discussion

The main results related to the hydrogen production will be discussed. The effects of the operating parameters such as current density, exchange current density, ohmic overvoltage and activation overpotential on the operating cell voltage have

also been discussed. All model equations related to the analysis are written in MATLAB editor and the results are validated against experimental data from the literature. The theoretical model and data have been analyzed in the MATLAB GUI. There are two cases that would affect the results. One is the temperature and the current density and the second one is the relation between the current density and the exchange current density. These conditions are divided into two cases and will be discussed in the next sub-topic.

There are three different values of exchange current density at anode and cathode which are represented as condition 1, 2 and 3 as shown in Table 3.

Table 3: Parameters value use for this analysis

Parameter	Condition		
	1	2	3
Exchange Current Density at Anode (A/cm <sup>2</sup> )	$1 \times 10^{-9}$	$5 \times 10^{-10}$	$1 \times 10^{-12}$
Exchange Current Density at Cathode (A/cm <sup>2</sup> )	$1 \times 10^{-3}$	$5 \times 10^{-4}$	$1 \times 10^{-4}$
Current Density (A/cm <sup>2</sup> )	0.1 : 0.1 : 2.0		

### **Case 1 – Temperature and current density relation**

Previous experimental manipulation usually focused on a different range of temperatures such as 40°C, 60°C and 80°C. The idea of using these parameter relations is to evaluate the value of voltage drop or voltage losses in an electrochemical cell whenever the temperature is increased. This phenomenon can be tested in terms of variation of the resistance conductivity against the temperature and also in the variety of operating cell voltage against the current density. Since this modeling uses the PEM, the presence of proton exchange is visible in the water electrolysis which means that the overpotential of the ohmic cannot be neglected. The process of calculating the operating cell voltage started with the sum of the reverse voltage with the activation overvoltage.

Figure 3 shows the polarization curve of the effect of temperature on the operating cell voltage. It can be observed that at a specified temperature, the operating cell voltage increases sharply at low current density and slowly thereafter with the current density. At 40°C and 2A/cm<sup>2</sup>, an operating voltage of 2.13V is achieved. However at higher temperature (80°C), the operating cell voltage drops to 1.98V at 2A/cm<sup>2</sup>. This constitutes about 7% reduction in operating cell voltage. The main parameter responsible for the voltage drop is the decrease in ohmic resistances as temperature increases. At high temperature, the ohmic resistance is decreased and this leads to the decrease in operating cell voltage. The effect of this result is that the operating cost of the electrolyzer decreases at higher temperatures due to lower power consumption.

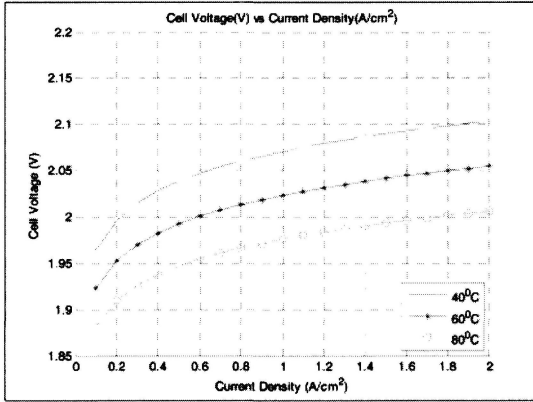


Figure 3: Effect of temperature on operating cell voltage

### Case 2 – Current density and exchange current density

Case 2 focuses on the sensitivity analysis of exchange current density at anode and cathode with respect to different temperature. The equation for activation overvoltage of anode and cathode below is the same as in Equation (12) and Equation (13) but are represented in different mathematical simplification. The activation overpotential at the anode is given according to Equation (32) [16]:

$$\eta_a = \frac{RT}{F} \sinh^{-1} \left( \frac{i_a}{2i_{o,a}} \right) \quad (32)$$

## Simulation Analysis Results

### Effect of temperature on resistance and conductivity of PEM

Figure 4 shows the effect of temperature on resistance and the conductivity. The results indicated that as temperature increases, there is a significant or sharp decrease in resistance from  $0.198\Omega/\text{cm}^2$  at  $40^\circ\text{C}$  to  $0.125\Omega/\text{cm}^2$  at  $80^\circ\text{C}$ . However there is a small increase in conductivity. From this observation it can be concluded that the ionic conductivity of the membrane assembly increases with temperature and this can lead to the increase in hydrogen flow rate.

The result of the simulation in Figure 4 showed similar agreement with the experimental result presented in Figure 5. Figure 4 shows the maximum value of the equivalent resistance is  $0.36\Omega/\text{cm}^2$  at  $40^\circ\text{C}$  while the minimum value is  $0.153\Omega/\text{cm}^2$  at  $80^\circ\text{C}$ . Even though both Figure 4 and 5 showed similar patterns, the MATLAB simulated resistance value has the lowest amount of resistance compared to the resistance value in the experiment.

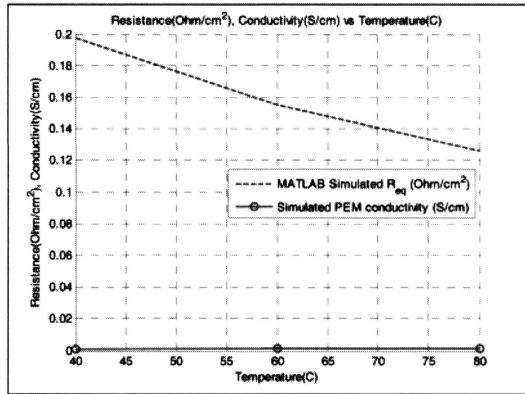


Figure 4: Variation of equivalent resistance and conductivity with temperature (Simulation)

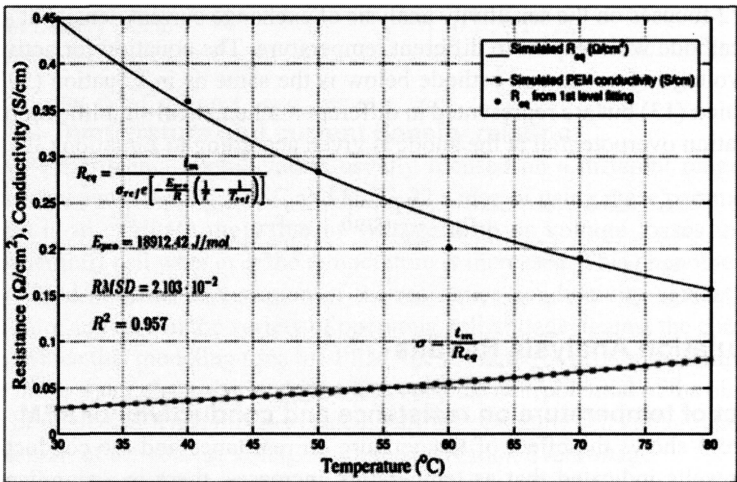


Figure 5: Equivalent resistance conductivity with temperature [13] (Experimental)

### Exchange current density effects

Figure 6 and 8 are the simulation results of the effect of exchange current density on operating cell voltage. For example Figure 6 shows that as the exchange current density at the anode decreases, the operating cell voltage increases and this result is obtained at a constant exchange current density at the cathode.

However the result showed that electrolysis system is able to operate at a lower operating cost when the exchange current density is bigger. A similar result is obtained for a variety of exchange current density at the cathode and constant exchange current density at anode. The difference between Figure 6 and 8 is that, the operating cell voltage 1.89V that corresponded to exchange current

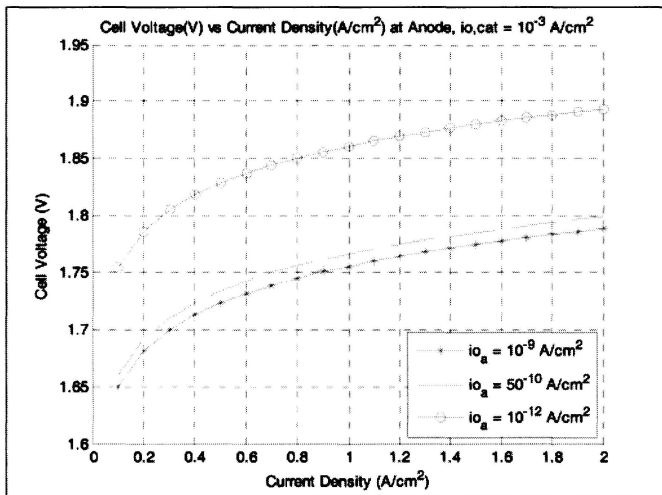


Figure 6: Effect of exchange current density at anode on cell voltage (Simulation)

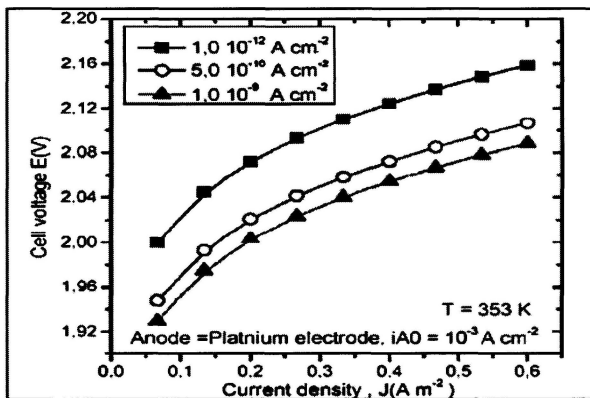


Figure 7: Effect of exchange current density at anode on cell voltage [15] (Experimental)

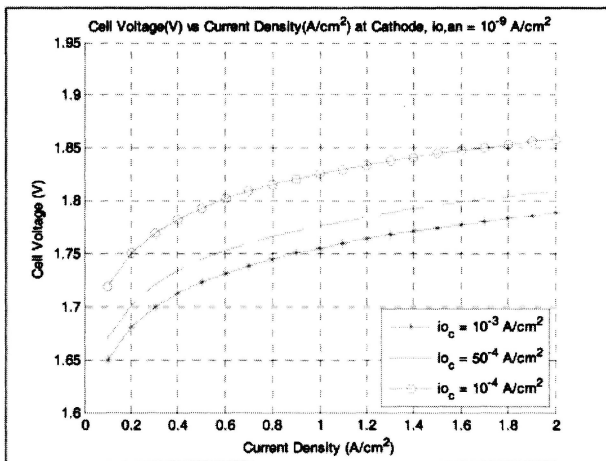


Figure 8: Effect of variation of exchange current density at cathode (Simulation)

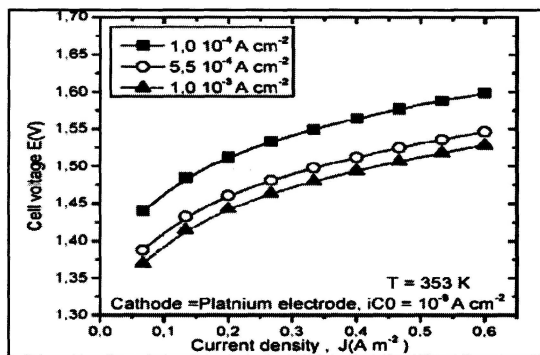


Figure 9: Effect of variation of exchange current density at cathode [15] (Experimental)

density of  $10^{-12} \text{ A/cm}^2$  is much higher compared with Figure 8 which operating cell voltage that corresponded to exchange current density of  $10^{-4} \text{ A/cm}^2$  is 1.86V and is bigger compared to the cathode.

We can conclude from the results that the amount of operating cell voltage at anode is much greater than at the cathode due to the oxidation effects at the anode. The results in Figures 6 and 8 followed similar agreement with experimental data from [15] as illustrated in Figure 7 and 9. All four figures showed the same pattern of proportional line at different conditions, however

it is clear that the anode reaction showed a slower reaction compared to the reaction at the cathode. The reason for these phenomena is because of the water dissociation occurred at anode and since the water molecules breaking phenomena occurred in anode site, it required a lot of power to break the water molecule into hydrogen charges and oxygen molecule.

### Voltage combination effect

In Figure 10, the simulation analyses showed the effectiveness for each overpotential with respect to the exchange current density. By plotting five different entities of the overpotential, the comparison can be made between the MATLAB simulation and experimental result reported by [15]. As shown in Figure 10, the reversible voltage remains constant as current density increases. The increases in ohmic overvoltage are relatively small as current density increases. The cathode overpotential increases steadily by a small amount due to the fast kinetic reaction on the cathode surface. The reaction at the anode is however slow and sluggish and the overall process is limited by the oxygen evaluation reaction.

This phenomenon causes the anode overpotential to increase faster at low current density and slowly increase after some time with current density. Comparing the anode and cathode reactions, it can be concluded that, the increase in the operating cell voltage ( $V_{cell}$ ) of the electrolysis cell is mainly because of the slow kinetics of the dissociation of water at the anode. As shown in Figure 10, an operating cell voltage of 2.58V is obtained at 1A/cm<sup>2</sup> and 80°C for Pt anode. In order to reduce the anode polarization effects, iridium-oxide (IrO<sub>2</sub>) is

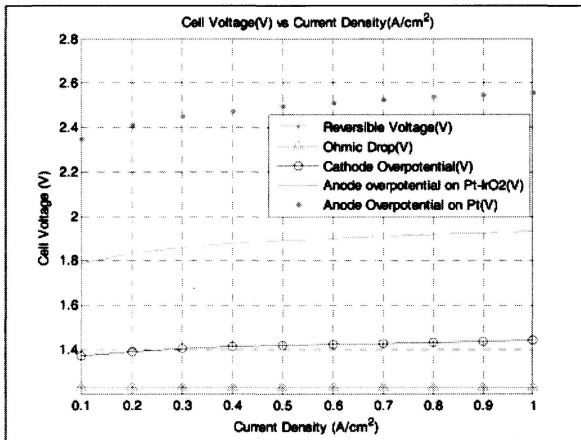


Figure 10: Simulation analysis of loss characteristics (overpotentials) affecting the model

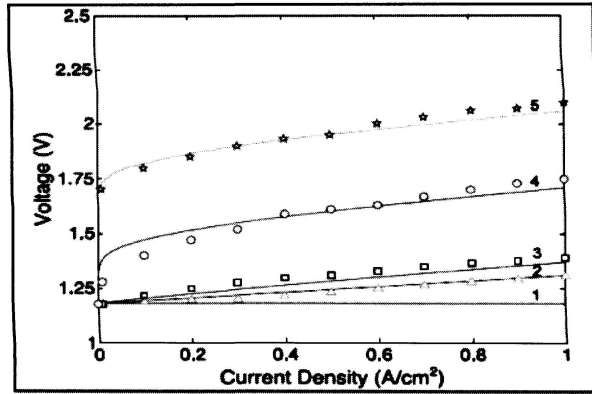


Figure 11: Loss characteristics (overpotentials) of the PEM model [15] (Experimental)

added. Similar to Pt. Ioroi et al. [17] who reported that the addition of IrO<sub>2</sub> to Pt at anode, can increase the efficiency of water electrolysis from 77% to 95% at 300 mA/cm<sup>2</sup>. Thus, with IrO<sub>2</sub>-Pt electrode at anode, the operating cell voltages decreased to 1.9V at 1A/cm<sup>2</sup> and 80°C. This is equivalent to 26.35% reduction in operating cell voltage. A comparison of the simulation result in Figure 10 is made with experimental results in Figure 11 and the two results showed similar agreement. The numeric 1,2,3,4 and 5 in Figure 11 corresponded to reversible voltage Ohmic overpotential, cathode overpotential, anode overpotential (IrO<sub>2</sub>-Pt) and anode overpotential (Pt) respectively.

### Electrochemical cell validation

Figure 12 shows the effect of different exchange current density at both anode and cathode on operating cell voltage. It can be shown that at a lower exchange current density for both anode and cathode, there is a corresponding increase in operating cell voltage. However when the exchange current density increased, the operating cell voltage decreases. The reason is being that the water dissociation at the anode side is much slower and therefore it needs higher exchange current density to initiate the reaction and when this condition is reached, the operating cell voltage decreases. On the other hand, when the exchange current density is smaller, the anode oxidation reaction requires a higher operating cell voltage.

Figure 13 shows the effect of exchange current density at the anode on power density. The power supply has a linear relation with current density, but there is little or no significant change in power supply to the PEM cell when the exchanger current density is changed. At 2 A/cm<sup>2</sup> and exchange current density of 10<sup>-12</sup> A/cm<sup>2</sup> a power of 3.75 W/cm<sup>2</sup> was observed, however this was reduced to 3.5 W/cm<sup>2</sup> at exchange current density of 10<sup>-9</sup> A/cm<sup>2</sup>.

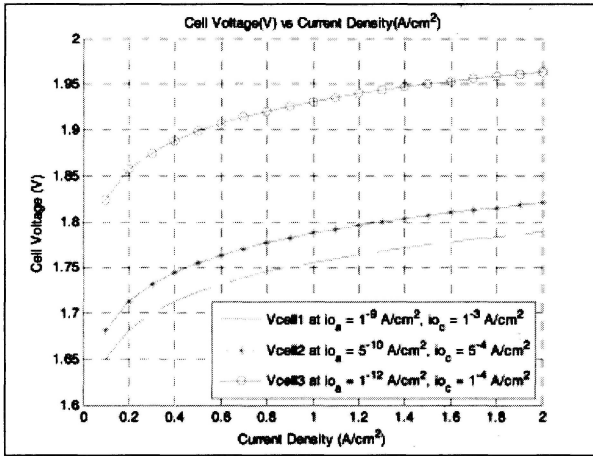


Figure 12: Effect of exchange current density on cell voltage polarization

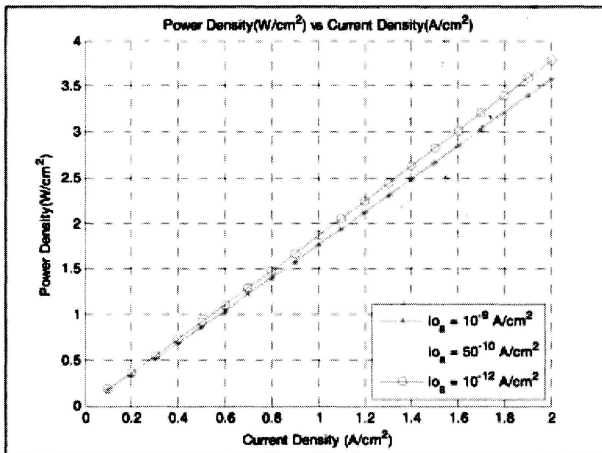


Figure 13: Variation analysis of power density effect at anode

## Conclusions

In this paper, different operating conditions such as exchange current density, temperature and current density have been analyzed for optimized hydrogen production of polymer electrolyte membrane electrolyzer system. It can be concluded from this paper that when the operating temperature of the electrolyzer

system increases, the ohmic resistance decreases. And this leads to the increase in ionic conductivity in the membrane. Therefore in order to increase the hydrogen flow rate, it is important to operate the electrolyzer system at the relatively high temperature.

## **References**

- [1] O. C. Onar, M. Uzunoglu and M. S. Alam. (2008). "Modeling, control and simulation of an autonomous wind turbine/photovoltaic/fuel cell/ultra-capacitor hybrid power system," *Journal of Power Sources*, 185, 1273-1283.
- [2] A. H. Abdol Rahim, A. S. Tijani, W. A. N. Wan Mohamed, S. Hanapi and K. I. Sainan. (2014). "An Overview of Hydrogen Production from Renewable Energy Source for Remote Area Application," *Applied Mechanics and Materials*, 699, 474-479.
- [3] "Hydrogen fact sheet," (2005). New York State Energy Research and Development Authority USA.
- [4] S. Koumi Ngoh and D. Njomo. (2012). "An overview of hydrogen gas production from solar energy," *Renewable and Sustainable Energy Reviews*, 16, 6782-6792.
- [5] J. Pettersson, B. Ramsey and D. Harrison. (2006). "A review of the latest developments in electrodes for unitised regenerative polymer electrolyte fuel cells," *Journal of Power Sources*, 157, 28-34.
- [6] S. Grigoriev, V. Porembsky and V. Fateev. (2006). "Pure hydrogen production by PEM electrolysis for hydrogen energy," *International Journal of Hydrogen Energy*, 31, 171-175.
- [7] S. Siracusano, V. Baglio, N. Briguglio, G. Brunaccini, A. Di Blasi, A. Stassi, R. Ornelas, E. Trifoni, V. Antonucci and A. S. Aricò. (2012). "An electrochemical study of a PEM stack for water electrolysis," *International Journal of Hydrogen Energy*, 37, 1939-1946.
- [8] F. Marangio, M. Pagani, M. Santarelli and M. Calì. (2011). "Concept of a high pressure PEM electrolyser prototype," *International Journal of Hydrogen Energy*, 36, 7807-7815.
- [9] V. Antonucci, A. Di Blasi, V. Baglio, R. Ornelas, F. Matteucci, J. Ledesma-Garcia, L. G. Arriaga and A. S. Aricò. (2008). "High temperature operation of a composite membrane-based solid polymer electrolyte water electrolyser," *Electrochimica Acta*, 53, 7350-7356.
- [10] C. Biaku, N. Dale, M. Mann, H. Salehfar, A. Peters and T. Han. (2008). "A semiempirical study of the temperature dependence of the anode charge transfer coefficient of a 6kW PEM electrolyzer," *International Journal of Hydrogen Energy*, 33, 4247-4254.

- [11] Y. F. Liu, Q. Su, H. Zhang and C. P. Cai. (2010). "Optimization of Photovoltaic-Electrolyzer System by Direct Coupling," *Applied Mechanics and Materials*, 44-47, 1578-1582.
- [12] K. Mazloomi, N. Sulaiman and H. Moayedi. (2012). "Electrical Efficiency of Electrolytic Hydrogen Production," *Int. J. Electrochem. Sci*,7, 3314-3326.
- [13] R. García-Valverde, N. Espinosa and A. Urbina, "Simple PEM water electrolyser model and experimental validation," *International Journal of Hydrogen Energy*, 37, 1927-1938 (2012).
- [14] L. Brahim, M. Bouziane and S. Lazhar. (2007). "Theoretical Investigation on Solid Polymer Electrolyte Water," *World International Hydrogen 2*, Ghardaïa, Algérie.
- [15] P. Choi. (2004). "A simple model for solid polymer electrolyte (SPE) water electrolysis," *Solid State Ionics*, 175, 535-539.
- [16] F. Marangio, M. Santarelli and M. Cali. (2009). "Theoretical model and experimental analysis of a high pressure PEM water electrolyser for hydrogen production," *International Journal of Hydrogen Energy*, 34, 1143-1158.
- [17] T. Ioroi, K. Yasuda, Z. Siroma, N. Fujiwara and Y. Miyazaki. (2002) "Thin film electrocatalyst layer for unitized regenerative polymer electrolyte fuel cells," *Journal of Power Sources*, 583-587.

# **JOURNAL OF MECHANICAL ENGINEERING (JMechE)**

## **Aims & Scope**

Journal of Mechanical Engineering (formerly known as Journal of Faculty of Mechanical Engineering) or JMechE, is an international journal which provides a forum for researchers and academicians worldwide to publish the research findings and the educational methods they are engaged in. This Journal acts as a vital link for the mechanical engineering community for rapid dissemination of their academic pursuits.

Contributions are invited from various disciplines that are allied to mechanical engineering. The contributions should be based on original research works. All papers submitted to JMechE are subjected to a reviewing process through a worldwide network of specialized and competent referees. To be considered for publication, each paper should have at least two positive referee's assessments.

## **General Instructions**

Manuscripts intended for publication in JMechE should be written in camera ready form with production-quality figures and done electronically in Microsoft Word 2000 (or above) and submitted online to [jmeche.int@gmail.com](mailto:jmeche.int@gmail.com). Manuscripts should follow the JMechE template.

All papers must be submitted online to [\*\*jmeche.int@gmail.com\*\*](mailto:jmeche.int@gmail.com)

Correspondence Address:

Editor In Chief  
Journal of Mechanical Engineering (JMechE)  
Faculty of Mechanical Engineering  
Universiti Teknologi MARA  
40450 Shah Alam, Malaysia.

Tel : 603 – 5543 6459

Fax : 603 – 5543 5160

Email: [jmeche.int@gmail.com](mailto:jmeche.int@gmail.com)

Website: <http://fkm.uitm.edu.my/jmeche>

# **Paper Title in Arial 18-point, Bold and Centered**

*Author-1*

*Author-2*

*Affiliation of author(s) from the first institution*

*Author-3*

*Affiliation of the author(s) from the second institution  
in Times New Roman 10 italic*

## **ABSTRACT**

*The first section of the manuscript should be an abstract, where the aims, scope and conclusions of the papers are shortly outlined, normally between 200 and 300 words. TNR-10 italic*

**Keywords:** *maximum 5 keywords.*

## **Title of First Section (Arial 11 Bold)**

Leave one blank line between the heading and the first line of the text. No indent on the first para after the title; 10 mm indent for the subsequent para. At the end of the section, leave two blank lines before the next section heading. The text should be right and left justified. The recommended font is Times New Roman, 10 points. In 152 mm x 277 mm paper size, the margins are: left and upper: 22 mm each; right: 20 mm, lower: 25 mm.

## **Secondary headings (Arial 10 Bold)**

The text starts in the immediately following line. Leave one blank line before each secondary heading.

## **Tertiary headings (Arial 10)**

If they are required, the tertiary headings shall be underlined. Leave one blank line before tertiary headings. Please, do not use more than three levels of headings, try to keep a simple scheme.

Tables and illustrations should be numbered with arabic numbers. Tables and illustrations should be centred with illustration numbers written one blank

Tables and illustrations should be numbered with arabic numbers. Tables and illustrations should be centred with illustration numbers written one blank line, centered, after the relevant illustration. Table number written one line, centered, before the relevant table. Leave two blank lines before the table or illustration. Beware that the proceedings will be printed in black and white. Make sure that the interpretation of graphs does not depend on colour. In the text, tables and figures should be referred to as Figure 1 and Table 1.

The International System of Units (SI) is to be used; other units can be used only after SI indications, and should be added in parenthesis.

Equations should be typed and all symbols should be explained within the manuscript. An equation should be preceded and followed by one blank line, and should be referred to, in the text, in the form Equation (1).

$$y = A + Bx + Cx^2 \quad (1)$$

Last point: the references. In the text, the references should be a number within square brackets, e.g. [3], or [4]–[6] or [2, 3]. The references should be listed in numerical order at the end of the paper.

Journal references should include all the surnames of authors and their initials, year of publication in parenthesis, full paper title within quotes, full or abbreviated title of the journal, volume number, issue number and pages.

Examples below show the format for references including books and proceedings

Examples of references:

- [1] M. K. Ghosh and A. Nagraj, "Turbulence flow in bearings," Proceedings of the Institution of Mechanical Engineers 218 (1), 61-4 (2004).
- [2] H. Coelho and L. M. Pereira, "Automated reasoning in geometry theorem proving with Prolog," J. Automated Reasoning 2 (3), 329-390 (1986).
- [3] P. N. Rao, Manufacturing Technology Foundry, Forming and Welding, 2nd ed. (McGraw Hill, Singapore, 2000), pp. 53-68.
- [4] Hutchinson, F. David and M. Ahmed, U.S. Patent No. 6,912, 127 (28 June 2005).